

TABLE I. Comparison of the 46.7- and 246-keV γ -ray transition probabilities with the Weisskopf single-particle estimate for $E2$ transitions

Transition	$T_{1/2}(\text{sec})^a$	α_t^b	$\tau_\gamma(\text{sec})$	$P_{\text{sp}}(\text{sec}^{-1})^c$	$P_{\text{obs}}(\text{sec}^{-1})$	$P_{\text{obs}}/P_{\text{sp}}$
46.7	$(29 \pm 6) \times 10^{-9}$	339	1.40×10^{-5}	2.4×10^4	7.0×10^4	2.9
246	$(1.8 \pm 0.2) \times 10^{-9}$	0.235	3.20×10^{-9}	9.8×10^7	3.1×10^8	3.2

^a Half-life of level from which transition proceeds.

^b Theoretical $E2$ total internal conversion coefficients obtained from reference 7.

^c Evaluated using a nuclear radius of $1.25 \times 10^{-12} A^{1/2}$ cm.

yielding a value of 38 ± 5 nsec. The observed transition probability (P_{obs}) for the 46.7-keV γ -ray transition then would be $5.3 \times 10^4 \text{ sec}^{-1}$ and $P_{\text{obs}}/P_{\text{sp}}$ would be 2.4. This

revised half-life value does not change the value of the 1.8 ± 0.2 nsec half-life obtained from the data shown in Fig. 1(A).

Polarization and Angular Distribution Measurements on the Neutrons from the $\text{Be}^9(p,n)\text{B}^9$ Reaction*

C. A. KELSEY,† G. P. LIETZ,‡ S. F. TREVINO, AND S. E. DARDEN
University of Notre Dame, Notre Dame, Indiana

(Received 1 June 1962; revised manuscript received 14 September 1962)

The polarization of the neutrons from the $\text{Be}^9(p,n)\text{B}^9$ reaction has been measured for laboratory emission angles of 30° , 50° , 70° , and 90° , for proton bombarding energies of 2.4, 2.75, 3.35, and 3.7 MeV. Angular distributions of the neutrons from this reaction have also been measured for nine proton bombarding energies between 2.5 and 4.1 MeV. For the polarization measurements, neutrons were scattered from analyzers of magnesium, oxygen, and carbon, and the asymmetries in the scattering were measured with the aid of an electromagnet which could rotate the polarization vector of the neutrons between the source and the scatterer. In detecting the neutrons, energy discrimination was employed to eliminate the effect of the three-body-breakup neutrons. The polarization is very small at 2.4 MeV, and at the higher energies is positive (Basel convention) at 30° , small at 50° , and negative at 70° and 90° . The largest value of the polarization found was 0.29 ± 0.04 at an emission angle of 30° and a bombarding energy of 3.7 MeV. Above 3.0-MeV proton energy the angular distributions show a broad maximum in the backward direction. Calculations of the cross section and polarization were made assuming the reaction involves only three levels in the compound nucleus. Although partially successful in reproducing the polarization data, these calculations were unable to reproduce the measured cross sections.

INTRODUCTION

PREVIOUS studies¹⁻⁵ of the $\text{Be}^9(p,n)\text{B}^9$ reaction indicate that there are resonances in the neutron yield at bombarding energies of 2.56, 3.5, and 4.6 MeV, corresponding to levels in B^{10} at excitation energies of 8.89, 9.7, and 10.7 MeV, respectively. The angular

distribution data of Marion,⁵ taken with a long counter, suggest that the two higher energy states are of opposite parity. Using isotopic spin considerations, Marion⁵ and Marion and Levin⁶ assigned spin and parity values of 3^+ , 2^+ , and 3^- to these levels in B^{10} . Recently Altman *et al.*⁷ have concluded that the 8.89 MeV level is more probably 3^- . Using a long counter, Albert *et al.*⁸ have measured the angular distribution of neutrons from both the $\text{Be}^9(p,n)\text{B}^9$ and the $\text{B}^{11}(p,n)\text{C}^{11}$ reactions. From a comparison of the results for the two reactions they conclude that these reactions very likely proceed largely through a direct interaction.

The measurements of Marion and Levin⁶ on the spectra of neutrons from the proton bombardment of

* Work supported in part by the Office of Naval Research.

† Present Address: Department of Physics, University of Wisconsin, Madison, Wisconsin. This article is based on a thesis submitted to the Graduate School of the University of Notre Dame by C. A. Kelsey in partial fulfillment of the requirements for the degree of Doctor of Philosophy.

‡ National Science Foundation Cooperative Fellow, 1961-62.

¹ H. T. Richards, R. V. Smith, and C. P. Browne, *Phys. Rev.* **80**, 524 (1950).

² H. T. Richards, M. W. Laubenstein, V. R. Johnson, F. Ajzenberg, and C. P. Browne, *Phys. Rev.* **81**, 316 (1951).

³ T. M. Hahn, C. W. Snyder, H. B. Willard, J. K. Bair, E. D. Klema, J. D. Kington, and F. P. Green, *Phys. Rev.* **85**, 934 (1952).

⁴ J. B. Marion, T. W. Bonner, and C. F. Cook, *Phys. Rev.* **100**, 91 (1955).

⁵ J. B. Marion, *Phys. Rev.* **103**, 713 (1956).

⁶ J. B. Marion and J. S. Levin, *Phys. Rev.* **115**, 144 (1959).

⁷ A. Altman, J. B. Marion, and W. M. MacDonald, *Bull. Am. Phys. Soc.* **6**, 225 (1961); *Nucl. Phys.* **35**, 85 (1962).

⁸ R. D. Albert, S. D. Bloom, and N. K. Glendenning, *Phys. Rev.* **122**, 862 (1961).

Be⁹ indicate that the cross section for the competing Be⁹(*p, p'*)Be⁸ process becomes appreciable above 3-MeV bombarding energy. Their data show the necessity for using energy discrimination in the neutron detector if one intends to eliminate the effects of these three-body-breakup neutrons. The angular distribution data of Anderson⁹ for the proton energy region between 3.5 and 10.9 MeV were taken with a time-of-flight apparatus and, hence, the effects of the three-body-breakup neutrons are absent from their data.

The polarization of the neutrons from this reaction has been measured at a laboratory emission angle of 45° by Cranberg¹⁰ for bombarding energies between 4.5 and 5.3 MeV, and in this laboratory¹¹ at 50° for proton energies between 2.4 and 4.4 MeV. For both measurements, energy discrimination was used to eliminate the low-energy continuum neutrons. The results of these experiments indicated small polarizations throughout the energy region investigated.

The present investigation was undertaken to obtain polarization data at other emission angles and angular distribution data relatively free of the effects of the three-body-breakup neutrons, and to see if these data can be understood simply in terms of the levels in B¹⁰ discussed above.

EXPERIMENTAL METHOD

Polarization Measurements

Neutrons were produced by bombarding beryllium targets, evaporated onto 20-mil tungsten disks, with protons from the Notre Dame electrostatic accelerator. Target thicknesses, determined by weighing the disks before and after the evaporation, ranged from 20 to 80 keV for 2-MeV protons. The thickness of several of these targets was checked by the rise curve method¹² and the two measurements always agreed within 10%.

Neutron polarizations were determined by measuring the asymmetry in scattering from various analyzers. A schematic top view of the experimental arrangement used to measure the asymmetries is shown in Fig. 1. An electromagnet was used to rotate the polarization vector of the neutron through 180° between the source and the scatterer. This method of measuring the asymmetry has been described previously¹³ and the present arrangement differs only in that the magnet has been completely surrounded by cast paraffin to increase the neutron shielding. The construction of inserts (see Fig. 1) for

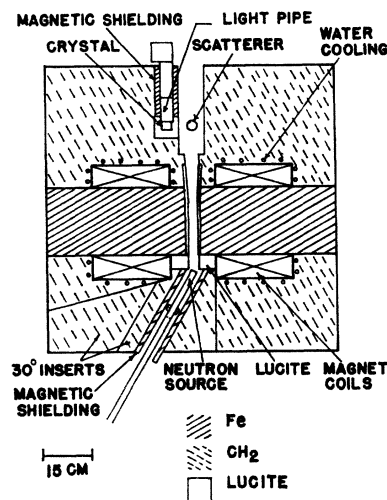


FIG. 1. A schematic top view of the spin-rotation magnet. The magnet is shown in the 30° emission-angle position.

each emission angle also served to reduce neutron background. In order to verify that the correct rotation of the polarization vector was produced by the magnetic field, the asymmetry in the scattering of polarized 280-keV neutrons by a magnesium analyzer was observed as a function of magnetic field. The results are shown in Fig. 2. The expected asymmetries, calculated from the known polarization¹⁴ of the incident neutrons, the measured value of the magnetic field, and the analyzing power of the magnesium scatterer,¹⁵ are given by the smooth curve. For these measurements, neutrons from the Li⁷(*p, n*)Be⁷ reaction, emitted at a laboratory angle of 70°, were used.

The polarization of the neutrons, P_1 , is related to the observed asymmetry, L/R , by the expression

$$P_1 P_2 = [(L/R) - 1] / [(L/R) + 1], \quad (1)$$

where L is the intensity of neutrons scattered into the detector with the magnet off, R is the intensity with the magnet on, and P_2 is the analyzing power of the scatterer.

Scatterers of magnesium, liquid oxygen, and carbon were used as polarization analyzers. The carbon and

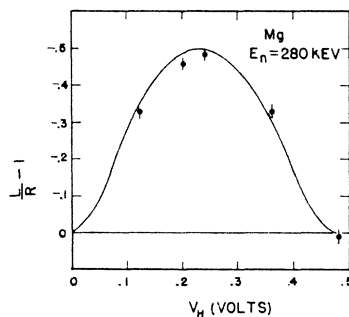


FIG. 2. The quantity $(L/R - 1)$ as a function of magnetic field. The abscissa is the voltage developed by the Hall probe used to measure the magnetic field. The curve was calculated from the known values of the polarization of the incident neutrons, the measured value of the magnetic field, and the analyzing power for the magnesium scatterer.

⁹ J. D. Anderson and C. Wong (private communication).

¹⁰ L. C. Cranberg, *Proceedings of the International Symposium on Polarization Phenomena of Nucleons* [Helv. Phys. Acta, Suppl. 6, 324 (1961)].

¹¹ C. A. Kelsey, T. R. Donoghue, and S. E. Darden, *Bull. Am. Phys. Soc.* 5, 404 (1960).

¹² R. Taschek and A. Hemmendinger, *Phys. Rev.* 74, 373 (1948).

¹³ S. E. Darden, C. A. Kelsey, and T. R. Donoghue, *Proceedings of the International Symposium on Polarization Phenomena of Nucleons*, [Helv. Phys. Acta, Suppl. 6, 269 (1961)].

¹⁴ S. M. Austin, S. E. Darden, A. Okazaki, and Z. Wilhelmi, *Nucl. Phys.* 22, 451 (1961).

¹⁵ A. J. Elwyn and R. O. Lane, *Nucl. Phys.* 31, 78 (1962).

magnesium samples were cylinders of the natural elements 3.7 and 3.3 cm in diameter and 10.0 and 5.5 cm in height, respectively. A thin-walled brass cylinder 2.5 cm in diameter, insulated with styrofoam, served as the liquid-oxygen container. The scattering samples were rigidly fixed to prevent motion when the magnetic field was turned on.

The analyzing power of oxygen was calculated using phase shifts obtained from the cross-section data of Striebel *et al.*¹⁶ and Okazaki.¹⁷ For magnesium, the analyzing power was obtained from the work of Elwyn and Lane.¹⁵ The analyzing power of carbon was calculated by Lane¹⁸ from a preliminary set of phase shifts chosen to give a satisfactory fit to all the available cross section and polarization data.

The scattered neutrons were detected by a stilbene crystal coupled to a 6810A photomultiplier tube by a light pipe, 6.6 cm long. Since stilbene is also an efficient detector of gamma radiation, a pulse shape discrimination technique was used to reduce background arising from gamma rays. Magnetic shielding around the phototube reduced the effects of the magnetic field on the gain of the phototube to a negligible amount. Periodic checks were made with a Pu-Be source to ensure that the magnetic shielding of the photomultiplier tube was adequate, and a further check against extraneous asymmetries was made by scattering 500-keV neutrons from carbon. Since at this neutron energy the analyzing power of carbon is less than 2%,¹⁵ this provides a sensitive test for the presence of spurious asymmetries.

In addition to gamma-ray discrimination in the neutron detector, energy discrimination was also used in order to eliminate pulses arising from low-energy neutrons. Two levels of energy discrimination were used in the polarization measurements, corresponding to approximately 50 and 75% of the incident neutron energy. On the basis of the published neutron spectra, the higher level of discrimination should be high enough to reduce the effect of the three-body-breakup neutrons to approximately 5% or less. The discrimination level was set by observing the recoil spectrum from the stilbene detector as recorded by a 256-channel analyzer and adjusting the bias level so that only pulses above the desired pulse height would be accepted. The technique of using two levels of energy discrimination enables one to determine the extent to which neglecting the contribution of the three-body-breakup neutrons is justified. If an appreciable number of three-body-breakup neutrons were being counted one would expect to measure different asymmetries with the two discrimination levels since the three-body-breakup neutrons almost certainly do not have the same polarization as the ground state neutrons. No such effect was found

since the measured asymmetries for both levels of discrimination agreed within statistics in all cases.

Typical source to scatterer distances were of the order of 50 cm, while typical scatterer-detector distances were approximately 10 cm. Background counting rates were determined by removing the scatterer and counting while collecting an amount of charge equal to that collected with the scatterer in place. Typical background counting rates ranged between 25 and 50% of the counting rate with the scatterer in place.

Angular Distribution Measurements

A hydrogen-filled proportional counter was used for the angular distribution measurements below 2.9-MeV proton energy since the low energy of the neutrons emitted in the backward direction made gamma discrimination with the stilbene detector very difficult. Above 3-MeV proton energy the stilbene crystal with gamma-ray discrimination was used. For some of the measurements, a target holder was used in which the target disk was held at 45° with respect to the proton beam direction. This target holder served to eliminate effects of attenuation in the target backing for emission angles near 90°. The detectors subtended an angle of about 4° at the neutron source. A determination of the variation with neutron energy of the efficiency of the stilbene detector was made by comparing the 0° yield of the $T(p,n)He^3$ reaction as measured with the stilbene crystal with the measured values¹⁹ of the 0° cross section. The relative efficiency of the recoil counter was determined by comparing its counting rate with that of a long counter for neutrons from the $Li^7(p,n)Be^7$ reaction. The cross-section data of Bevington *et al.*²⁰ were used to correct for the presence of the second group of neutrons from this reaction.

Two energy discrimination levels were chosen for the measurements with the stilbene crystal, corresponding to 50% of the maximum pulse heights observed at neutron emission angles of 0° and 80° in the laboratory system. For the recoil counter measurements two energy discrimination levels were used, corresponding to 50% of the maximum pulse height observed for laboratory emission angles of 0° and 150°. The back angle data were joined to the forward angle data in their region of overlap near 90°. Background counts were measured by placing a paraffin cone between the source and the detector. Typical magnitudes of the background were approximately 5% of the direct counting rate. The experimental data were corrected for background and energy variation of detector efficiency, and were converted to the center-of-mass system. Except at the two highest energies, the data were normalized to a 0° yield curve measured with

¹⁶ H. R. Striebel, S. E. Darden, and W. Haeberli, Nucl. Phys. **6**, 188 (1958).

¹⁷ A. Okazaki, Phys. Rev. **99**, 55 (1955).

¹⁸ R. O. Lane (private communication).

¹⁹ J. D. Seagrave, in *Proceedings of the Conference on Nuclear Forces and the Few-Nucleon Problem, London, 1959*, edited by T. C. Griffith and E. A. Power (Pergamon Press, New York, 1960).

²⁰ P. R. Bevington, W. W. Rolland, and H. W. Lewis, Phys. Rev. **121**, 871 (1961).

the proportional counter. Above 3.5 MeV the 0° yield curve of Marion and Levin⁶ was used for normalization. Both yield curve measurements were made with energy sensitive detectors to eliminate the effects of the three-body-breakup neutrons and are in excellent agreement. The absolute efficiency of the proportional counter was determined by comparing its counting rate with that of a long counter for neutrons from the $\text{Li}^7(p,n)\text{Be}^7$ reaction. A Pu-Be source of known strength was used to measure the absolute efficiency of the long counter.

The detector was rotated about the beryllium target by a remote control motor and the position of the detector was monitored by a closed circuit television set. The position of the detector was reproducible to $\pm 1^\circ$.

RESULTS

Polarizations

The measured asymmetries were corrected for multiple scattering in the sample and for the variation in azimuthal scattering angle arising from the finite height of the sample. For the multiple scattering correction, the procedure discussed by Darden *et al.*²¹ was used. The polarizations were then obtained from the corrected asymmetries using Eq. (1). To obtain the average value of P_2 , the analyzing powers of the scatterers were averaged over energy and angle, weighing appropriately with the differential cross section. Results of the polarization measurements are listed in Table I. The headings of the first six columns in the table are the average incident proton energy, \bar{E}_p ; the average neutron energy, \bar{E}_n ; the energy spread of the neutrons, ΔE_n ; the laboratory emission angle of the neutrons, ψ ; the laboratory scattering angle of the neutrons, ϑ ; and the analyzer used. The remaining columns give the measured asymmetries L/R with their associated statistical uncertainties, the uncorrected values of P_1P_2 , the corrected values of P_1P_2 , the average analyzing power \bar{P}_2 , and the polarization of the neutrons P_1 . The sign of the polarization follows the Basel convention.

Uncertainties indicated in the seventh column are statistical only, while those in the last column include in addition the uncertainty introduced by the multiple

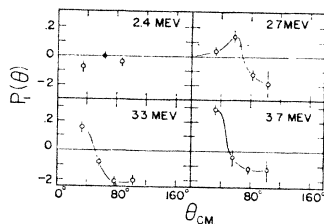


FIG. 3. The angular distribution of polarization of the neutrons from the $\text{Be}^9(p,n)\text{B}^9$ reaction for four proton bombarding energies. The proton bombarding energy is indicated in the upper right-hand corner of each figure. The abscissa is the c.m. emission angle. Curves have been drawn through the points to emphasize the trend of the data.

scattering correction, but do not include the uncertainty associated with the analyzing power, P_2 . It has been pointed out²² that the uncertainty in the calculated analyzing power is difficult to estimate, since the accuracy of the analyzing power is related in a complicated way to the uncertainties in the measured cross sections. Consequently, relatively little is known about the uncertainty in the calculated polarizations, $P_2(\vartheta)$. The estimated probable uncertainty in the analyzing powers of the scatterers used in this experiment is approximately ± 0.07 .

Inspection of Table I shows that at 30° emission angle the polarization is small for low energies and rises to approximately 0.30 at 3.7-MeV bombarding energy. There appears to be no appreciable polarization at 50° emission angle throughout the energy region investigated, but at 70° emission angle the polarization is negative. At 90° emission angle the polarization is also negative over most of the energy region covered. The angular dependence of the polarization for four bombarding energies is shown in Fig. 3. The curves through the data points have been drawn to emphasize the trend of the data. There is considerable similarity in the shapes of the angular distributions at the two higher energies.

Angular Distributions

The results of the angular distribution measurements are illustrated in Fig. 4, where the curves for the various proton energies have been displaced vertically an amount $\Delta\sigma$ for clarity. The estimated relative uncertainty of 8% includes the statistical uncertainty, the uncertainty in the determination of the relative efficiency of the detector, and an estimated uncertainty of about 5% arising from the contribution of the three-body-breakup neutrons. A conservative estimate would place the absolute uncertainties in the cross section near 20%. Below 3-MeV proton energy the shapes of the angular distributions agree with the published angular distributions of Marion,⁵ taken with

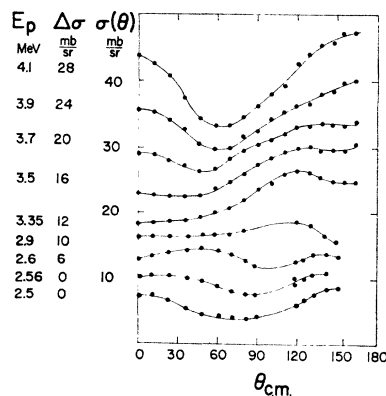


FIG. 4. The angular distributions of neutrons from the $\text{Be}^9(p,n)\text{B}^9$ reaction. Cross sections per unit solid angle and emission angles are given in the c.m. system. The proton bombarding energy refers to the laboratory system. The curves have been displaced an amount $\Delta\sigma$ for clarity.

²¹ S. E. Darden, T. R. Donoghue, and C. A. Kelsey, Nucl. Phys. **22**, 439 (1961).

²² W. Haerberli, *Fast Neutron Physics* [Interscience Publishers, Inc., New York (to be published)], Part II, Chap. VG.

TABLE I. Measured asymmetries, analyzing powers, and polarizations of the $\text{Be}^9(p,n)\text{B}^9$ neutrons.

\bar{E}_p (MeV)	\bar{E}_n (keV)	ΔE_n (keV)	ψ (deg)	ϑ (deg)	Ana- lyzer	Measured L/R	P_1P_2	Corrected P_1P_2	$\bar{P}_2(\vartheta)$	P_1
2.377	396	42	30	60	O ₂	0.947±0.021	-0.027±0.010	-0.065±0.028	0.69	-0.094±0.041
2.380	404	42	30	60	O ₂	0.978±0.030	-0.011±0.015	-0.026±0.048	0.56	-0.047±0.085
2.712	747	42	30	60	O ₂	0.970±0.021	-0.015±0.010	-0.016±0.011	-0.41	0.039±0.027
3.395	1428	42	30	120	O ₂	0.771±0.018	-0.129±0.011	-0.131±0.011	-0.86	0.157±0.013
3.685	1715	29	30	120	C	1.18 ±0.018	0.078±0.010	0.104±0.014	0.37	0.29 ±0.04
4.136	2157	31	30	120	C	1.18 ±0.012	0.078±0.010	0.104±0.014	0.70	0.14 ±0.02
2.290	255	50	50	90	Li	0.880±0.10	-0.065±0.064	-0.087±0.072	-0.33	0.26 ±0.22
2.407	378	27	50	60	O ₂	1.027±0.050	0.013±0.024	0.006±0.010	0.94	0.006±0.01
2.45	420	50	50	90	O ₂	0.998±0.042	-0.001±0.021	-0.001±0.020	0.90	-0.001±0.02
2.54	510	35	50	90	O ₂	0.983±0.078	-0.008±0.039	-0.009±0.039	-0.30	0.030±0.13
2.56	550	120	50	90	O ₂	1.085±0.051	0.041±0.025	0.045±0.021	-0.28	-0.160±0.076
2.58	580	35	50	90	O ₂	1.092±0.050	0.044±0.024	0.051±0.027	-0.31	-0.160±0.088
2.64	600	50	50	90	O ₂	0.923±0.033	-0.040±0.017	-0.050±0.018	-0.25	0.203±0.070
2.67	630	35	50	90	O ₂	0.965±0.041	-0.018±0.021	-0.020±0.023	-0.22	0.090±0.10
2.750	712	27	50	60	O ₂	0.930±0.021	-0.036±0.010	-0.038±0.011	-0.29	0.131±0.038
2.79	800	50	50	60	O ₂	1.015±0.042	0.007±0.021	0.007±0.021	-0.47	-0.015±0.045
2.93	941	50	50	60	O ₂	0.962±0.039	-0.019±0.020	-0.020±0.020	-0.96	0.021±0.021
3.004	984	27	50	60	O ₂	1.075±0.032	0.036±0.015	0.048±0.020	-0.82	-0.058±0.014
3.08	1075	50	50	60	O ₂	1.050±0.050	0.024±0.024	0.030±0.024	0.53	0.056±0.045
3.32	1260	120	50	60	O ₂	0.844±0.038	-0.085±0.021	-0.082±0.022	0.66	-0.125±0.034
3.353	1275	27	50	60	O ₂	0.947±0.014	-0.027±0.007	-0.040±0.010	0.59	-0.068±0.017
3.698	1597	27	50	120	C	0.97 ±0.028	-0.015±0.014	-0.017±0.015	0.325	-0.052±0.046
3.91	1800	50	50	125	C	0.965±0.028	-0.020±0.017	-0.018±0.017	0.41	-0.044±0.041
4.13	2000	50	50	125	C	1.061±0.045	0.034±0.025	0.044±0.028	0.40	0.11 ±0.08
4.17	2040	50	50	125	C	1.084±0.074	0.047±0.042	0.061±0.048	0.30	0.20 ±0.16
4.34	2200	50	50	125	C	0.953±0.037	-0.030±0.024	-0.031±0.029	0.70	-0.04±0.039
2.380	294	42	70	90	Mg	1.049±0.020	0.023±0.010	0.023±0.010	-0.57	-0.040±0.018
2.712	586	42	70	60	O ₂	1.084±0.027	0.040±0.013	0.041±0.013	-0.29	-0.14 ±0.045
2.756	625	30	70	60	O ₂	1.060±0.020	0.029±0.010	0.030±0.010	-0.27	-0.11 ±0.037
3.350	1143	30	70	60	O ₂	0.813±0.029	-0.103±0.015	-0.106±0.016	0.72	-0.15 ±0.022
3.350	1143	30	70	60	O ₂	0.726±0.020	-0.159±0.012	-0.165±0.013	0.72	-0.230±0.017
3.353	1146	27	70	60	O ₂	0.775±0.020	-0.127±0.011	-0.132±0.011	0.71	-0.186±0.016
3.363	1154	32	70	60	O ₂	0.736±0.023	-0.152±0.013	-0.158±0.013	0.72	-0.22 ±0.018
3.573	1337	30	70	90	O ₂	1.16 ±0.017	0.074±0.079	0.080±0.090	-0.72	-0.11 ±0.012
3.726	1473	30	70	90	O ₂	1.117±0.020	0.056±0.009	0.060±0.010	-0.50	-0.120±0.020
3.741	1483	30	70	90	O ₂	1.118±0.022	0.056±0.009	0.060±0.010	-0.50	-0.120±0.020
3.756	1498	42	70	120	O ₂	1.216±0.051	0.099±0.023	0.107±0.025	-0.75	-0.14 ±0.033
3.842	1572	30	70	120	C	0.893±0.024	-0.056±0.013	-0.089±0.019	0.31	-0.29 ±0.063
2.754	532	27	90	60	O ₂	1.070±0.034	0.034±0.017	0.035±0.017	-0.18	-0.19 ±0.095
3.317	982	27	90	60	O ₂	1.298±0.039	0.13 ±0.017	0.14 ±0.018	-0.68	-0.205±0.026
3.702	1290	27	90	120	C	0.957±0.029	-0.022±0.015	-0.028±0.017	0.215	-0.13 ±0.08
2.455	450	42	30	90	C	1.005±0.010				
2.50	630	35	50	90	C	0.992±0.025				
2.560	430	42	70	90	C	1.010±0.013				
2.846	760	32	70	90	C	0.992±0.016				
2.827	581	27	90	90	C	0.999±0.026				

a long counter, except at 2.56-MeV bombarding energy, where the present data show a larger dip near 90° and a larger rise in the backward direction. At 3.5-MeV bombarding energy the cross sections⁵ measured with a long counter have shapes similar to the present data; however, the magnitudes of the present cross sections are smaller. This discrepancy can probably be attributed to the presence of three-body-breakup neutrons. A comparison of the present angular distributions with the published long counter data of Albert *et al.*⁸ is difficult since their data do not extend to emission angles greater than 120°. However the forward peak present in their curves for energies of 3.4 MeV and above, does not appear in the present data until 3.5 MeV. It is difficult to explain this difference in shape unless the distribution of the three-body-breakup

neutrons is peaked strongly in the forward direction at these energies. The data of Anderson,⁹ taken with a time-of-flight apparatus give an angular distribution for 3.5-MeV proton energy in agreement with that shown in Fig. 4, except that the backward peak in the present data is slightly higher.

Above 2.9-MeV proton energy one feature common to all the curves is the peak in the backward direction. This peak increases in magnitude and moves in the backward direction with increasing bombarding energy.

DISCUSSION

An attempt was made to reproduce the polarization and angular distribution data assuming compound nuclear levels at excitation energies of 8.89, 9.7, and

10.7 MeV with spins and parities of 3^- , 2^+ , and 3^- , respectively. The formulas used to calculate the cross sections and polarizations were obtained from the general expressions which have been given by Blatt and Biedenharn,²³ and Simon and Welton.²⁴ In carrying out the calculations several simplifying assumptions were made. These assumptions are:

(a) The channel radius was assumed to be independent of channel spin and to be the same for $p+Be^9$ as for $n+B^9$.

(b) The ratio of neutron reduced width to proton reduced width is independent of channel spins.

(c) In the incident and exit channels, orbital angular momentum (l) values greater than two do not contribute significantly in the energy region under consideration.

(d) The two 3^- levels do not interfere appreciably with each other.

While there is no strong experimental evidence for or against the first and second assumptions, they seem to be reasonable first approximations for calculations intended merely to produce a qualitative fit to the data. The channel radius was taken to be 4.3 F. Orbital angular momenta greater than $l=2$ were not considered, since conservation of parity requires that the l values involved in forming a level differ by two units of orbital angular momentum, and in this energy region the penetrability factor for f waves is at least an order of magnitude smaller than for p waves, and the penetrability for g waves is at least an order of magnitude smaller than for d waves. The last assumption was made since the two 3^- levels are separated by 2 MeV and do not appear to overlap appreciably. Any attempt to obtain a detailed fit to the data would probably have to take into account the interference between the two 3^- states.

Since both Be^9 and B^9 have ground-state spins and parities of $\frac{3}{2}^-$, the use of assumption (c) means that only the value, $l=1$, will be involved in the formation and decay of the 2^+ state in B^{10} , and only the value, $l=2$, for the 3^- states. Both channel-spin states can contribute to the formation of all three compound states involved. In addition to the channel radius, resonance energies, and reduced proton and neutron widths in the two channel spin states, the relative phases between the various reduced width amplitudes and the alpha-decay widths for the two upper levels were included as

²³ J. M. Blatt and L. C. Biedenharn, Rev. Mod. Phys. **24**, 258 (1952).

²⁴ A. Simon and T. A. Welton, Phys. Rev. **90**, 1036 (1953).

parameters in the calculation. The contributions of the $Be^9(p,p'n)Be^8$ and $Be^9(p,p')Be^{9*}$ channels were not included explicitly, since only a qualitative fit to the data was being sought. In varying the parameters involved in the calculations, the requirement was imposed that a qualitative fit to the 0° excitation curve be achieved before the more complicated polarization and angular distribution calculations be attempted. Several calculations using various mixtures and phases of channel spin states for a given level were tried to test the sensitivity of the cross section and polarization to mixtures of channel spin. Although it was possible to reproduce qualitatively the angular distributions of polarizations at 3.3 and 3.7 MeV by proper choice of parameters, no combination of parameters was found which would fit simultaneously the angular distribution and polarization data. Consequently, it did not seem promising to pursue these calculations further.

If any of the aforementioned assumptions were relaxed, permitting more parameters to be varied, agreement might be achieved. However the limited amount of data available might not insure a unique fit. It is also possible that this reaction proceeds, to some extent, by way of a direct interaction. The low binding energy of the last neutron in the Be^9 nucleus suggests that a direct interaction might be an important mechanism even at these relatively low bombarding energies.

CONCLUSIONS

The results of the polarization measurements indicate that the $Be^9(p,n)B^9$ reaction may have some usefulness as a source of polarized neutrons above about 3.5-MeV bombarding energy provided adequate energy discrimination is used to eliminate the effects of the three-body-breakup neutrons. Assuming the reaction proceeds via the three compound nuclear states discussed, a satisfactory fit to the polarization and angular distribution data was not achieved using the simplifying assumptions listed above.

ACKNOWLEDGMENTS

The authors wish to thank Dr. J. D. Anderson and Dr. C. Wong for communicating their results to us, and Dr. H. W. Lefevre for the design of the gamma-ray discrimination circuit. We would also like to express our appreciation to Dr. R. O. Lane for the calculations of the analyzing power of carbon.